

# Inelastic neutron scattering of hydrogen and butyronitrile adsorbed on Raney-Co catalysts

Adam Chojceki<sup>1,\*</sup>, Hervé Jobic<sup>2</sup>, Andreas Jentys<sup>1</sup>, Thomas E. Müller<sup>1</sup>, and Johannes A. Lercher<sup>1</sup>

<sup>1</sup>*Institut für Technische Chemie II, Technische Universität München, Lichtenbergstraße 4, 85747 Garching, Germany*

<sup>2</sup>*Institut de Recherches sur la Catalyse, CNRS 2 Avenue Albert Einstein, 69626 Villeurbanne, France*

Received 16 June 2002; accepted 25 June 2004

Inelastic Neutron Scattering (INS) spectroscopy was used to characterize the catalytic hydrogenation of butyronitrile on the surface of parent and LiOH-modified Raney-Co. At low pressure hydrogen is mainly adsorbed on 3-fold sites. Co-adsorbed butyronitrile and hydrogen react on the unmodified Raney-Co sample to several partially hydrogenated products that contain N–H bonds. The nature of the species suggests that bi-molecular condensation leading to N-Butylidene-1-butanamine is feasible.

**KEY WORDS:** butyronitrile; INS; LiOH; Raney-Cobalt; surface modification; surface species.

## 1. Introduction

Raney type catalysts are formed by leaching of aluminum from binary or multi-component alloys of catalytically active transition metals (typically Cu, Ni, Co) and promoters (such as Cr, Fe, Mo) [1]. Raney cobalt catalysts are used commercially for hydrogenation reactions such as the reduction of nitriles to primary amines with H<sub>2</sub> [2]. Although the elementary steps of this reaction on the metal surface have not been studied *in situ*, it is generally assumed that it proceeds step-wise *via* imines or other partially hydrogenated intermediates [3–5]. These intermediates are susceptible to nucleophilic condensation, which lead to the formation of Schiff bases and enamines that can be further hydrogenated to secondary and tertiary amines [6]. As a consequence, unsatisfactory selectivities to primary amines (due to the formation of secondary and tertiary amines) are frequently observed.

In the absence of ammonia, which is generally used as solvent in industrial practice, the thermodynamic equilibrium predicts low concentrations of primary amines (< 1 mol % for the hydrogenation of butyronitrile [7]). In general, high selectivity to primary amines requires to enhance the rate of the hydrogenation of unsaturated C–N groups [8, 9]. Own preliminary experiments have shown that Raney-Co modified with LiOH is an excellent catalyst for the selective hydrogenation of butyronitrile leading to almost 100% n-butylamine [10].

In order to characterize the surface chemistry occurring during the hydrogenation of butyronitrile on the surface of Raney-Co and LiOH-modified Raney-Co, Inelastic Neutron Scattering (INS) was used in combination with *ab initio* theoretical calculations to support the

assignment of the vibrations of the adsorbed molecules. INS is particularly useful, as the vibrational modes that involve hydrogen motions in the molecules are much more intense because of the significantly larger incoherent scattering cross section of <sup>1</sup>H compared to the other elements and isotopes (including <sup>2</sup>H) [11]. Therefore, INS has been used successfully for the characterization of hydrogen adsorption and hydrogenation reactions on the transition metal surfaces [12–15].

## 2. Experimental

### 2.1. Sample preparation

Raney-Co (GRACE Davison Chemical Division of W.R. Grace & Co grade # 2700 lot # 7865) with the chemical composition 1.85 wt% Al; 97.51 wt% Co; 0.3 wt% Fe and 0.34 wt% Ni was used. The catalyst (212 g) was washed with de-ionized water until the pH of 7 was reached. The volatiles were removed in vacuum (< 4 mbar) and the catalyst was dried at 323 K for 10 h. Doping with LiOH was carried out in an aqueous solution of LiOH (3.254 g in 100 cm<sup>3</sup> de-ionized water, treatment at room temperature for 1 h followed by drying in vacuum at 323 K, 10 h. The concentration of Li<sup>+</sup> in LiOH doped Raney-Co was 0.5 wt% as determined with AAS (UNICAM 939 AA-Spectrometer). Pre-dried Raney-Co catalysts, both parent and LiOH-modified ( $m_{\text{cat}} = 25$  g), were placed inside aluminum containers used for INS experiments under inert atmosphere. Note that the specific surface areas of the parent and the LiOH-modified Raney-Co, determined by N<sub>2</sub> adsorption after activation in vacuum at 473 K for 1 h, were 24.5 and 14.8 m<sup>2</sup> · g<sub>cat</sub><sup>−1</sup>, respectively. For INS the catalysts were activated in vacuum ( $p \leq 10^{-6}$

\*To whom correspondence should be addressed.

mbar) at 473 K for 6 h. For reference measurements, samples of activated Raney-Co and LiOH doped Raney-Co were used. H<sub>2</sub> was adsorbed on one Raney-Co sample with a pressure of 0.2 bar. On samples of parent and LiOH-doped Raney-Co 13.0 and 9.4 mmol of butyronitrile were adsorbed first (to achieve the same surface coverage according to the specific surface area) and the samples were subsequently equilibrated with 0.2 bar H<sub>2</sub>.

## 2.2. INS measurements

Experiments were carried out at 10 K at the Be-filter detector spectrometer IN1BeF at ILL in Grenoble using the Cu (220) monochromator. The instrument resolution was between 25 cm<sup>-1</sup>, at low energy transfers and 50 cm<sup>-1</sup> at high energy transfers. Note that the Be-filter energy shift of 40 cm<sup>-1</sup> was subtracted from all spectra presented. Additionally, reference spectra of solid butyronitrile (Aldrich) and from an empty aluminum container were recorded.

## 2.3. Data treatment

The vibrational modes of hydrogen adsorbed on different cobalt clusters were computed using Dmol<sup>3</sup> (version 4.2.1, Accelrys Inc.) [16]. Cobalt clusters consisting of 4–5 atoms were created based on the bulk crystal structure of hexagonal close-packed cobalt (hcp Co). Calculations on the sorption structures of hydrogen in one to 4-fold coordination sites included the minimization of a hydrogen atom over the cobalt surface atoms (at fixed coordinates), followed by the computation of the vibrational frequencies of the system in the optimized geometry. The generalized gradient approximation (gga) density functional theory method (DFT) with Perdew-Wang 1991 (p91) Hamiltonian and double numeric basis functions including polarization functions (dnp) in expansion of molecular orbitals were used. In order to meet the self consistent field (SCF) convergence criteria electronic state was set on “thermal”, which allows electrons to be smeared out among all orbitals within in the vicinity of the Fermi level. Note that the crystal structure of cobalt up to 693 K is hexagonal close-packed [17] with dominant crystal morphologies of (100), (101) and (002) planes (40.8, 39.6 and 19.6 % of the facet area, respectively) [18]. For butyronitrile, n-butylamine and butylideneimine a *ab initio* quantum mechanical calculations with the B3LYP hybrid functional and a 6-31G\*\* basis set followed by a Møller-Plesset correlation energy correction truncated at second-order (MP2) were done using GAUSSIAN 98 [19]. The INS spectra were calculated from the theoretical frequency and amplitude results using aCLIMAX [20]. No scaling procedures were applied; however, the computed spectra were subjected to a Fourier smoothing procedure for an easier comparison with the experimental spectra.

## 3. Results and discussion

The INS spectra of the activated parent Raney-Co of the parent catalyst after adsorption of hydrogen and of the activated LiOH-modified Raney-Co are shown in Figures 1 a, b and c, respectively.

Contributions of the phonon vibrations of the Co hcp crystal lattice would be expected in the INS spectrum below 300 cm<sup>-1</sup> (at approximately 250, 200, and 133 cm<sup>-1</sup> [21]), but were not observed. The broad range of scattering contributions between 450 and 1200 cm<sup>-1</sup> with two distinct peaks at 685 and 766 cm<sup>-1</sup> are assigned to residual hydrogen which remained on the sample after the activation procedure. Above 1200 cm<sup>-1</sup> the spectrum did not show any peaks. After adsorption of H<sub>2</sub> on the parent Raney-Co, the scattering increased and a number of small peaks at 250, 560, 638, 782, 895, 1104 and ~1660 cm<sup>-1</sup> were observed. The spectrum of LiOH

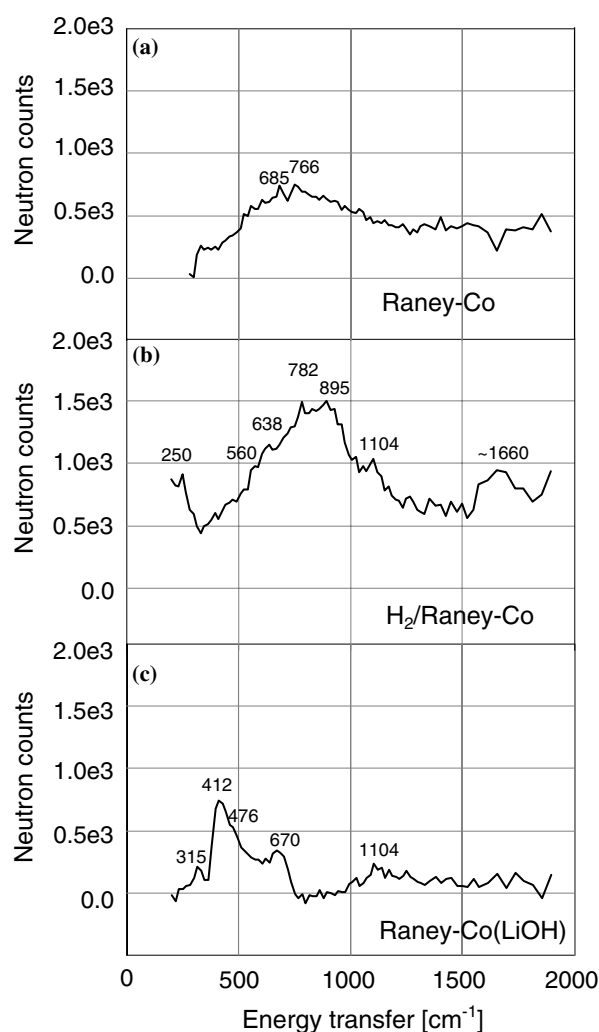


Figure 1. (a) INS spectrum of activated Raney-Co after subtraction of INS spectrum of Al-container, (b) INS spectrum of activated Raney-Co equilibrated with H<sub>2</sub> (0.2 bar) after subtraction of the INS spectrum of activated Raney-Co, (c) INS spectrum of activated LiOH-modified Raney-Co after subtraction of INS spectrum of activated Raney-Co.

Table 1  
Assignment of hydrogen vibrations modes on Raney-Co and Raney-Ni

Hydrogen Adsorption On Raney-Co		Hydrogen Adsorption On Raney-Ni	
INS [ $\text{cm}^{-1}$ ]	Description	INS [ $\text{cm}^{-1}$ ]	Description
~250	Hydrogen on 4-fold sites with D4h symmetry (i.e., 101 plane); Co <sub>4</sub> -H symmetric stretching vibrations.		
~573	Hydrogen on 3-fold sites with C3v symmetry (i.e., 001 plane); Co <sub>3</sub> -H antisymmetric stretching vibrations.	~600	The symmetric stretching of $\mu_4$ -H species adsorbed on (100) facets
~637	Hydrogen on 3-fold sites with C3v symmetry (i.e., 101 plane); Co <sub>3</sub> -H antisymmetric stretching vibrations. Probably some contribution from 4-fold sites ("hollow sites") with D4h symmetry: Co <sub>2</sub> -H antisymmetric stretching vibrations.		
~782	Hydrogen on 3-fold sites with C3v symmetry (i.e., 101 plane); Co <sub>2</sub> -H asymmetric stretching vibrations.	~800	The antisymmetric stretching of $\mu_3$ -H species adsorbed on (110) facets
~894	Hydrogen on 3-fold sites with C3v symmetry (i.e., 001 plane); Co <sub>2</sub> -H antisymmetric stretching vibrations.	~940	The antisymmetric stretching of $\mu_3$ -H species adsorbed on (111) facets
~1100	Hydrogen on 3-fold sites with C3v symmetry (i.e., 001 and 101 planes); Co <sub>3</sub> -H symmetric stretching vibrations.	~1100	The symmetric stretching of $\mu_3$ -H species adsorbed on (110) facets
		~1130	The symmetric stretching of $\mu_3$ -H species adsorbed on (111) facets
~1660	Probably hydrogen on some 1-fold sites. However, the DFT calculations of single bound hydrogen on 101 and 001 planes yield a peak at 1800–1860 $\text{cm}^{-1}$	~1800	The stretching vibrations of $\mu_1$ -H species (on-top hydrogen); the bending mode is expected between 800 and 1130 $\text{cm}^{-1}$ , and is thus hidden by the more intense features due to multiply bound hydrogen

modified Raney-Co showed peaks at 315, 412 (with a shoulder at 476) and at 670  $\text{cm}^{-1}$ .

After adsorption of hydrogen on Raney-Co, mainly multiply-bound hydrogen was observed. The various adsorption complexes of hydrogen on Raney-Co on the basis of DFT-calculated vibration modes of hydrogen on different cobalt surfaces are compiled in Table 1. For comparison, an assignment of hydrogen adsorbed on Raney-Ni is included [22].

At low pressures, sorption of hydrogen onto Raney-Co occurs mainly at 3-fold sites (corresponding to maxima at 782, 895 and 1100  $\text{cm}^{-1}$ ) with small contributions of "on-top" hydrogen, although this sorption mode can be prevailing at a high hydrogen pressure.

The wet deposition of LiOH onto Raney-Co surface and the subsequent activation procedure at 473 K may lead to a number of lithium (surface) compounds. Most likely, the surface reaction of lithium hydroxide monohydrate (LiOH·H<sub>2</sub>O) with bayerite (aluminum hydroxide found on the surface of Raney catalysts) leads to the formation of lithium dialuminate (Li<sub>2</sub>Al<sub>2</sub>(OH)<sub>7</sub>·2H<sub>2</sub>O) [23]. Structural water can be removed from Li<sub>2</sub>Al<sub>2</sub>(OH)<sub>7</sub>·2H<sub>2</sub>O below 473 K [24], whereas the crystal water of LiOH·H<sub>2</sub>O(s) is removed already at ~380 K

[25]. Thus, dehydrated lithium hydroxide and small amounts of lithium aluminates are speculated to exist on the surface of LiOH doped Raney-Co. LiOH crystallizes in the tetragonal symmetry group  $D_{4h}^7 \equiv P4/nmm$  and each Bravais cell contains two formula units of LiOH [26, 27]. The internal and external fundamental vibrations are classified into five symmetry species of the  $D_{4h}^7$  group (i.e.,  $a_{1g}$ ,  $e_g$ ,  $b_{1g}$ ,  $a_{2u}$ ,  $e_u$ ) [28]. The IR and Raman vibrational active modes have been studied in detail [29–32] and a high-temperature study of polycrystalline LiOH by INS has been presented by Safford and LoSacco [33]. The observed bands in the INS spectrum of LiOH deposited on Raney-Co mainly contains vibrations involving motions of the OH<sup>−</sup> group such as the translational lattice vibrations (i.e.,  $T'(\text{OH}^-)$ ) of the  $a_{1g}$  species at 315  $\text{cm}^{-1}$ , which are observed in Raman and INS spectra of polycrystalline LiOH at 329 and 332  $\text{cm}^{-1}$ , respectively. The very strong INS vibration at 412  $\text{cm}^{-1}$  is attributed to the rocking lattice mode of OH<sup>−</sup> ( $R'(\text{OH}^-)$ ) of the  $e_u$  symmetry species (419  $\text{cm}^{-1}$  in IR spectrum). The adjacent, less intense INS vibration (shoulder at 476  $\text{cm}^{-1}$ ) probably reveals a translational lattice vibration  $T'(\text{OH}^-)$  of the  $a_{2u}$  species. However, the literature data on this vibration are conflicting. The IR data by Yoshida and Hase refer to a

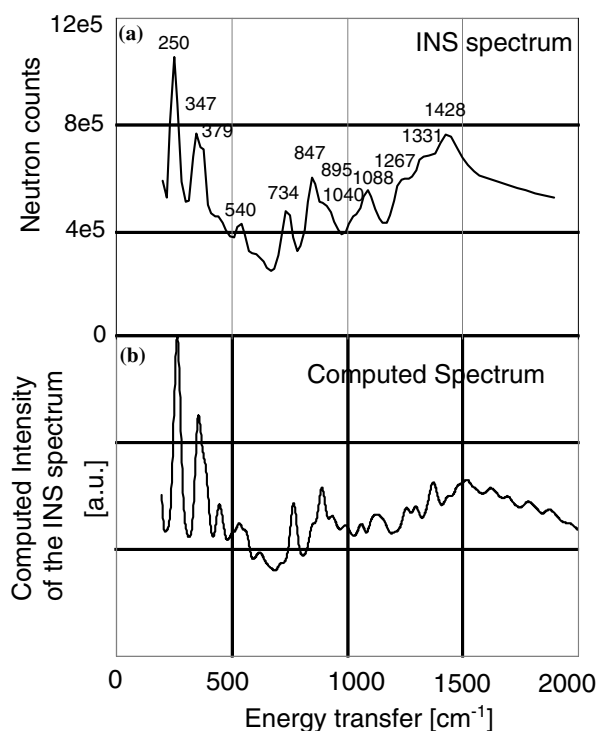


Figure 2. (a) Observed and (b) calculated INS spectrum of butyronitrile. The calculated INS spectrum is a linear combination of the computed INS spectra of *gauche* (0.75) and *anti* (0.25) conformers of butyronitrile.

vibration at  $595\text{ cm}^{-1}$  as the coupled vibration of  $T'(OH^-)$  and  $T'(Li^+)$   $a_{2u}$  species [34, 35]. On the other hand, Buchanan *et al.* have reported a vibration at

$495\text{ cm}^{-1}$  as the IR active vibration of the  $a_{2u}$  symmetry species [32]. Also, [33] Safford and LoSacco have presented the INS spectrum of LiOH with an intense peak at  $468\text{ cm}^{-1}$ . The vibration at  $670\text{ cm}^{-1}$  in the INS spectrum is assigned to the pure rotational vibration of  $OH^-$  groups of the  $e_g$  species. The  $R'(OH^-)$  with a contribution from the mechanical coupling with  $T'(Li^+)$  was observed at  $620\text{ cm}^{-1}$  in the Raman spectrum and corresponds to the INS band at  $625\text{ cm}^{-1}$  of LiOH. Note that the acoustic lattice vibrations of LiOH and the internal stretching modes of  $OH^-$  are expected to appear outside the energy scale of the INS spectrum considered (i.e., below  $200$  and above  $3000\text{ cm}^{-1}$ , respectively).

The vibrational assignment of butyronitrile based on IR and Raman spectra, and *ab initio* calculations has been comprehensively studied by Durig *et al.* [36]. The comparison of the INS spectrum of butyronitrile and the computed one is presented in Figure 2 and the assignment of the peaks observed is compiled in Table 2.

A conformational search and analysis, followed by a forcefield minimization procedure yielded only two stable conformers, i.e., *gauche* and *anti* [37]. A good reproduction of the experimental spectrum using a combination of INS spectra of both conformers indicates that both were present in the solid sample of butyronitrile with the *gauche* form the more abundant conformer.

The INS spectra of co-adsorbed butyronitrile and hydrogen on parent (a) and LiOH-modified Raney-Co (c) are shown in Figure 3 (after subtraction of the

Table 2

Assignment of the vibrational frequencies [ $\text{cm}^{-1}$ ] for *gauche* and *anti*-conformers of butyronitrile. (In parenthesis the results of the *ab initio* study presented Durig *et al.* [36])

Vibration no.	Description of the vibrations of a butyronitrile molecule $CH_3CH_2^*CH_2C\equiv N$	DFT calculated frequencies for the butyronitrile conformers		Observed INS vibrations
		<i>gauche</i>	<i>anti</i>	
$\nu_9$	$CH_3$ antisymmetric deformation	1522 (1571)	1566 (1571)	
$\nu_{10}$	$CH_3$ antisymmetric deformation	1515 (1566)	1559 (1565)	
$\nu_{11}$	$CH_2$ deformation ("the scissoring bend")	1504 (1555)	1551 (1558)	
$\nu_{12}$	$^*CH_2$ deformation ("scissoring bend" conjugation with the nitrile group)	1479 (1534)	1527 (1536)	1428
$\nu_{13}$	$CH_3$ symmetric deformation ("umbrella bend")	1434 (1481)	1469 (1476)	
$\nu_{14}$	$CH_2$ wag	1381 (1420)	1434 (1437)	1331
$\nu_{15}$	$^*CH_2$ wag	1364 (1403)	1338 (1343)	
$\nu_{16}$	$CH_2$ twist	1295 (1332)	1367 (1369)	1267
$\nu_{17}$	$^*CH_2$ twist	1258 (1293)	1300 (1304)	
$\nu_{18}$	$CH_3$ rock	1130 (1166)	1151 (1154)	
$\nu_{19}$	$CH_2$ rock	1104 (1140)	899 (905)	
$\nu_{20}$	$^*C-C-C$ antisymmetric stretch	1061 (1103)	1096 (1097)	1040
$\nu_{21}$	$\equiv C-^*C$ stretch	932 (958)	984 (986)	895
$\nu_{22}$	$^*CH_2$ rock	888 (913)	1162 (1168)	
$\nu_{23}$	$^*C-C-C$ symmetric stretch	848 (880)	906 (909)	847
$\nu_{24}$	$CH_2$ rock	770 (792)	761 (766)	734
$\nu_{25}$	$N\equiv C-^*C$ bend	563 (563)	521 (526)	540
$\nu_{26}$	$N\equiv C-^*C$ bend	388 (378)	367 (376)	379
$\nu_{27}$	$^*C-C-C$ bend	354 (361)	350 (354)	347
$\nu_{28}$	$CH_3$ torsion	267 (276)	252 (254)	250

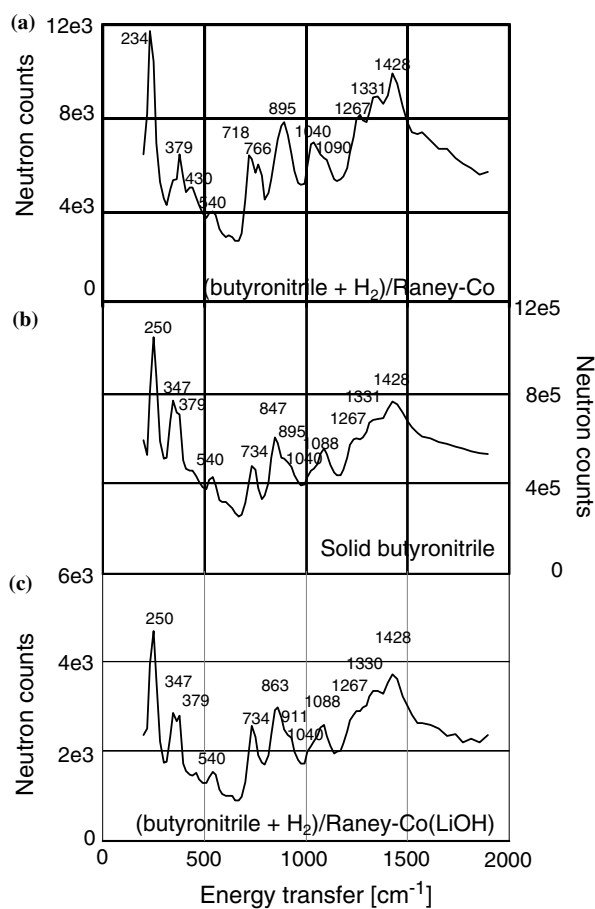


Figure 3. INS spectra of co-adsorbed butyronitrile and hydrogen on (a) parent and (c) LiOH-modified Raney-Co after subtraction of the reference background. The INS spectrum of a solid sample of butyronitrile (b) is included for comparison.

reference backgrounds). The INS spectrum of solid butyronitrile (b) is included for comparison.

(The intensity of the INS spectrum of solid butyronitrile was two orders of magnitude higher than those of

the other two spectra due to the higher amount of material exposed to the beam). Different INS spectra of co-adsorbed butyronitrile and hydrogen were obtained for the parent and the LiOH-modified Raney-Co. The latter resembled closely the INS spectrum of butyronitrile. Only the peak at  $863\text{ cm}^{-1}$  (with the shoulder at  $911\text{ cm}^{-1}$ ) appeared at slightly higher wavenumbers compared to the peak at  $847\text{ cm}^{-1}$  (with the shoulder at  $895\text{ cm}^{-1}$ ) in the INS spectrum of solid butyronitrile. In contrast, the INS spectrum of butyronitrile and hydrogen co-adsorbed on the parent catalyst showed several new and shifted peaks. The doublet at  $347$  and  $379\text{ cm}^{-1}$  in the INS spectrum of solid butyronitrile was replaced by bands at  $379\text{ cm}^{-1}$  and  $430\text{ cm}^{-1}$  (low intensity). The band at  $734\text{ cm}^{-1}$  of solid butyronitrile was replaced by two peaks at  $718$  and  $766\text{ cm}^{-1}$  and the asymmetric peak at  $847\text{ cm}^{-1}$  with a shoulder at  $895\text{ cm}^{-1}$  of butyronitrile, was replaced by a fairly symmetric peak at  $895\text{ cm}^{-1}$ . Above  $1200\text{ cm}^{-1}$ , all three spectra were fairly similar (i.e., bands appeared at  $1428$ ,  $1331$  and  $1267\text{ cm}^{-1}$ ), which might indicate that the hydrocarbon part of butyronitrile does not significantly interact with the surface of the Raney-Co catalysts.

Adsorbed hydrogen and butyronitrile are expected to react to partially hydrogenated species on the cobalt surface. As the INS spectrum observed after co-adsorption of butyronitrile and hydrogen on LiOH-doped Raney-Co was identical to the INS spectrum of solid butyronitrile, we conclude, however, that hydrogenation of adsorbed butyronitrile did not occur. In this context, it is important to note that a prolonged induction period was observed with LiOH-doped Raney-Co during the catalytic hydrogenation of butyronitrile [10]. The lower pressure used during the INS experiment does not allow to rule out that the induction period that has been extended over the whole period, when the samples were studied. The only indication that butyronitrile undergoes a reaction on

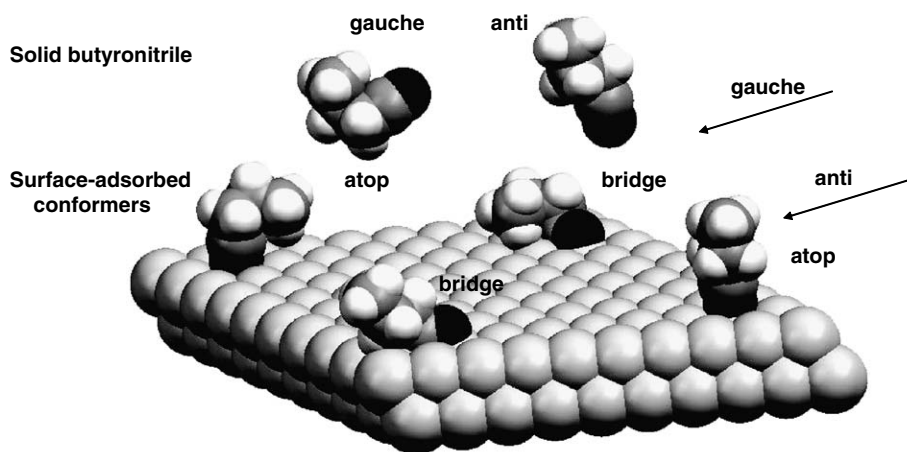


Figure 4. Schematic presentation of the possible (atop and bridge) interaction of butyronitrile with the (001) plane of cobalt. Note that conformational analysis allowed to accommodate both gauche and anti conformers on the surface.

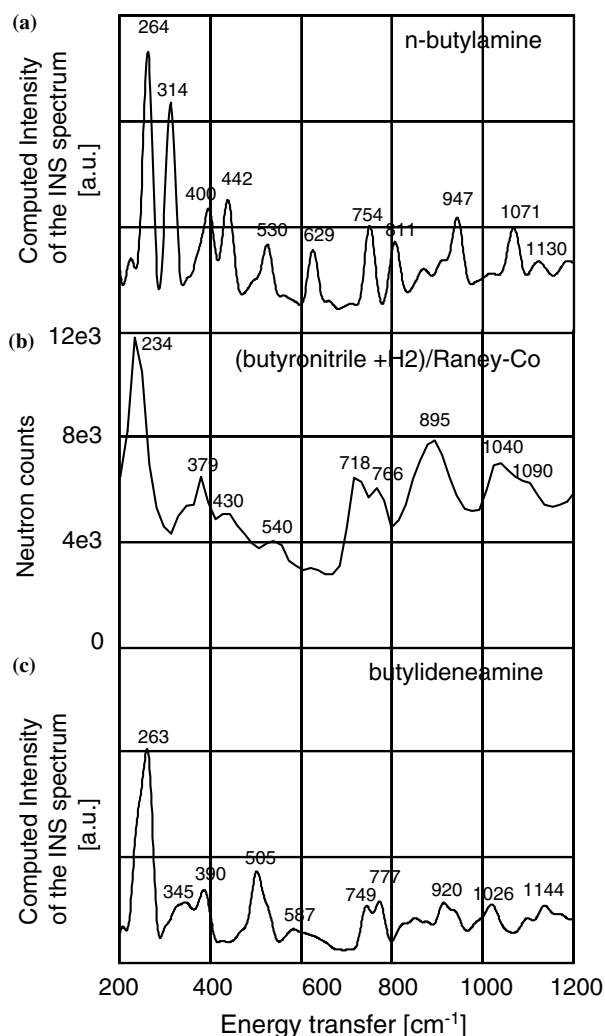


Figure 5. Comparison of the INS spectrum of (b) co-adsorbed butyronitrile and hydrogen on the parent catalysts with the *ab initio* computed spectra of (a) butylamine and (c) butylideneimine.

the surface is a shift of the peak at  $847\text{--}863\text{ cm}^{-1}$  (the shoulder is shifted from  $895$  to  $911\text{ cm}^{-1}$ ), which could indicate that a higher proportion of butyronitrile molecules is present on the modified surface in the

*anti* conformer resulting from a repulsive interaction of the hydrocarbon part with the modified surface. Possible structures for butyronitrile chemisorbed *via* the  $\text{C}\equiv\text{N}$  group on the (001) plane of hexagonal cobalt are shown in Figure 4 (resulting from energy minimization using the Universal Force Field [38]).

The N–H wagging and twisting vibrations in the INS spectrum of co-adsorbed butyronitrile and hydrogen on the parent Raney-Co catalyst indicate the presence of partially hydrogenated butyronitrile. In addition, the large peak at  $\sim 895\text{ cm}^{-1}$  points to the presence of co-adsorbed atomic hydrogen on the 3-fold sites. In order to assign the surface species, the spectrum (Figure 5, b) was compared with computed spectra of n-butylamine (a) and butylideneimine (c), the products of full and partial hydrogenation of butyronitrile, respectively.

The computed spectrum of butylideneimine better reproduces the experimental data. Especially, the two overlapping peaks observed in the experimental spectrum at  $718$  and  $766\text{ cm}^{-1}$  were also present in the computed INS spectrum of butylideneimine at  $749$  and  $777\text{ cm}^{-1}$ , while similar but slightly more separated peaks were calculated for the INS spectrum of butylamine (at  $754$  and  $811\text{ cm}^{-1}$ ). This doublet indicates a motion of one or two hydrogen atoms attached to the nitrogen atom (i.e., wagging and twisting vibrations).

The step-wise hydrogenation of the nitrile group on the metal surface may proceed *via* a number of surface-adsorbed species (see Figure 6). The selectivity to primary amines is high as long as the probability of condensation of the electrophilic carbon with nitrogen nucleophiles forming a new C–N bond remains low. In this respect, a low surface coverage in reactive species and a protection of the reactive carbon are important.

If the hydrogenation preferentially occurs *via* nitrenes (Figure 6a), the carbon center becomes saturated first during the step-wise hydrogenation. After the addition of the second hydrogen, atom condensation is no longer possible. Furthermore, nitrene species are bound strongly to the metal center and would be non-reactive for condensation reactions. Probably, condensation

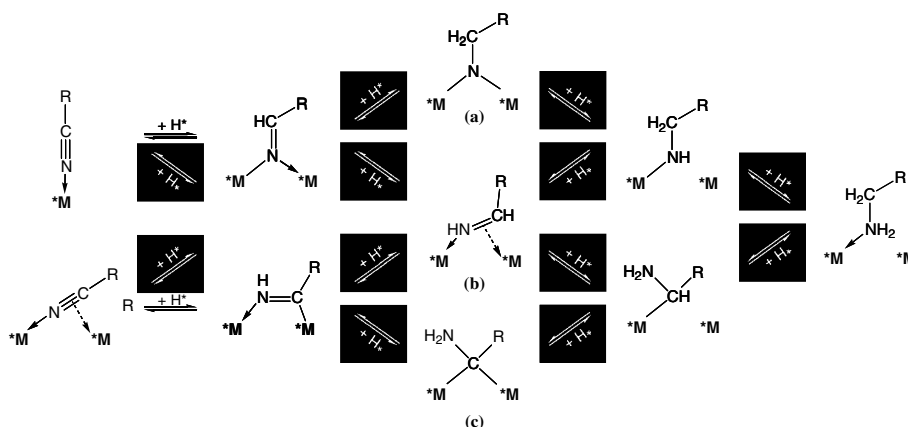


Figure 6. Possible surface reactions for the hydrogenation of butyronitrile ( $\text{R}=(\text{CH}_2)_2\text{CH}_3$ ).

reactions occur mainly *via* carbene species having a highly reactive electrophilic carbon center where nucleophilic attack by a (partially hydrogenated) nitrogen atom can occur (Figure 6c). The spectroscopic evidence on N–H groups in the surface intermediates suggests the presence of such carbenes on the cobalt surface. Obviously, the condensation reaction between carbenes or between carbene and amine can lead to *N*-butylidenebutan-1-amine. The formation of imines on the surface cannot be ruled out at this stage (Figure 6b).

On the other hand, the alkali-doped cobalt surface probably leads to stronger adsorption of nitrogen species. As a consequence, the nitrile is preferentially adsorbed perpendicular to the surface. Also, the transition states of the nitrene route are lowered in energy. Both effects lead to an enhanced (relative) reactivity of the carbon atom for hydrogenation. It is concluded that the nitrene route dominates in case of the LiOH-doped catalyst.

#### 4. Conclusions

Sorption of hydrogen on Raney-Co at low pressure mainly occurs on the 3-fold sites. Wet deposition of LiOH on Raney-Co and subsequent temperature treatment at 473 K generate clusters of LiOH on the cobalt surface. On parent Raney-Co, butyronitrile and hydrogen react promptly to partially hydrogenated intermediates characterized by the presence of N–H bonds. Condensation reactions between these species appear likely. LiOH modification of Raney-Co leads to modified sorption properties. It is speculated that strong binding *via* the nitrogen atom may stimulate fast hydrogenation of the carbon atom in the nitrile group, which prevents secondary condensation reactions. However, further experimental evidence is necessary to clarify the nature of the species populating the surface of LiOH-doped Raney-Co during the reaction.

#### Acknowledgment

Prof Dr Winfried Petry is gratefully thanked for the discussion of the results. Institut Laue-Langevin is thanked for access to the IN1-BeF spectrometer and, in particular, Alexander Ivanov for assistance during the INS experiments. A sample of Active Raney-Co grade # 2700 lot # 7865 was kindly donated by Unichema Chemie GmbH, Emmerich, Germany. Wolfgang Kaltner is thanked for proofreading the manuscript.

#### References

- [1] M.S. Wainwright in: *Preparation of Solid Catalysts*, (eds) G. Ertl, H. Knözinger and J. Weitkamp (Wiley-VCH, Weinheim, 1999) pp. 28–43.
- [2] M.G. Turcotte and T.A. Johnson in: *Kirk-Othmer Encyclopedia of Chemical Technology*, Vol.2, (ed.) J.I. Kroschwitz (John Wiley & Sons (NY, 1992, 4th ed.) pp. 369–386.
- [3] P.R. Rylander in: *Hydrogenation Methods*, (Academic Press (London, 1988, 2nd ed.) pp. 94–103.
- [4] B. Coq, D. Tichit and S. Ribet, *J. Catal.* 189 (2000) 117.
- [5] F.J.G. Alonso, M.G. Sanz and V. Riera, *Organometallics* 11 (1992) 801.
- [6] Y. Huang and W.M.H. Sachtler, *Appl. Catal. A* 182 (1999) 365.
- [7] HSC Chemistry for Windows 5.1., Outokumpu Research Oy, P.O. Box 60, FIN–28101 Pori, Finland, Fax: +358–2–626–5310; Phone: +358–2–626–6111
- [8] F. Medina, P. Salagre and J.E. Sueiras, *J. Mol. Cat.* 81 (1993) 363.
- [9] H. Greenfield, *Ind. Eng. Chem. Prod. Rev. Dev.* 6 (1967) 142.
- [10] A. Chojceki in: *Selective Hydrogenation of Butyronitrile over Raney-Metals*, Ph.D. Thesis (TU-München, (2004).
- [11] B.S. Hudson, *J. Phys. Chem. A* 105 (2001) 3949.
- [12] D. Graham, J. Howard and T.C. Waddington, *J. Chem. Soc., Faraday Trans. 1* 79 (1983) 1281.
- [13] H. Jobic and A. Renouprez, *J. Chem. Soc., Faraday Trans. 1* 80 (1984) 1991.
- [14] J.M. Nicol, *Spectrochim. Acta* 48A (1992) 313.
- [15] F. Hochard, H. Jobic, G. Clugnet, A. Renouprez and J. Tomkinson, *Catal. Lett.* 21 (1993) 381.
- [16] B. Delley, *J. Chem. Phys.* 92 (1990) 508.
- [17] B. Strauss, F. Frey, W. Petry, J. Trampenau, K. Nicolaus, S.M. Shapiro and J. Bossy, *Phys. Rev. B* 54 (1996) 6035.
- [18] J.D. Donnay and G. Harker, *Am. Mineral.*, 22 (1937) 446 ; Particles morphology was computed Cerius<sup>2</sup> program suite using Crystal Builder and Surface Builder modules (Accelrys Inc, 2001).
- [19] M.J. Frisch, G.W. Trucks, H.B. Schlegel, G.E. Scuseria, M.A. Robb, J.R. Cheeseman, V.G. Zakrzewski, J.A. Montgomery, R.E. Stratmann, J.C. Burant, S. Dapprich, J.M. Millam, A.D. Daniels, K.N. Kudin, M.C. Strain, O. Farkas, J. Tomasi, V. Barone, M. Cossi, R. Cammi, B. Mennucci, C. Pomeli, C. Adamo, S. Clifford, J. Ochterski, G.A. Petersson, P.Y. Ayala, Q. Cui, K. Morakuma, D.K. Malick, A.D. Rabuck, K. Raghavachari, J.B. Foresman, J. Cioslowski, J.V. Ortiz, B.B. Stefanov, G. Lui, A. Liashenko, P. Piskorz, I. Komaromi, R. Gomperts, R.L. Martin, D.J. Fox, T. Keith, M.A. Al-Laham, C.Y. Peng, Nanayakkara, C. Gonzalez, M. Challacombe, P.M.W. Gill, B.G. Johnson, W. Chen, M.W. Wong, J.L. Andreas, M. Head-Gordon, E.S. Repolgle and J.A. Pople, *GAUSSIAN 98* (Revision A.9) (1998) Gaussian, Pittsburg, PA.
- [20] aCLIMAX v. 4.0, the new software for analyzing and interpreting INS spectra; J.A. Ramirez-Cuesta, to be published
- [21] N. Wakabayashi, R.H. Schrem and H.G. Smith, *Phys. Rev. B* 25 (1982) 5122.
- [22] F. Hochard, H. Jobic, J. Massardier and A. Renouprez, *J. Mol. Catal. A* 95 (1995) 165.
- [23] J.P. Thiel, C.K. Chiang and K.R. Poeppelmeier, *Chem. Mater.* 5 (1993) 297.
- [24] M. Nayak, T.R.N. Kutty, V. Jayaraman and G. Periaswamy, *J. Mater. Chem.* 7 (1997) 2131.
- [25] J.M. Kiat, G. Boemare, B. Rieu and D. Aymes, *Solid State Commun.* 108 (1998) 24.
- [26] T. Ernst, *Z. Phys. Chem. B20* (1933) 65.
- [27] H. Dachs, *Z. Kristallogr.* 112 (1959) 60.
- [28] K.A. Wickersheim, *J. Chem. Phys.* 31 (1959) 863.
- [29] Y. Hase and I.V. Pagotto-Yoshida, *Chem. Phys. Lett.* 65 (1979) 46.
- [30] F. Harbach and F. Fisher, *J. Phys. Chem. Solids* 36 (1975) 601.
- [31] I.V.P. Yoshida and Y. Hase, *Spectrosc. Lett.* 12 (1979) 409.
- [32] A. Buchanan, H.H. Caspers and H.R. Marlin, *J. Phys. Chem.* 40 (1964) 1125.
- [33] G.J. Safford and F.J. LoSacco, *J. Chem. Phys.* 44 (1966) 345.
- [34] I.V.P. Yoshida and Y. Hase, *Spectrosc. Lett.* 12 (1979) 409.
- [35] Y. Hase and I.V.P. Yoshida, *J. Mol. Struct.* 56 (1979) 297.

- [36] J.R. Durig, B.R. Drew, A. Koomer and S. Bell, Phys. Chem. Chem. Phys. 3 (2001) 766.
- [37] Conformational search using modeling and simulation environment Cerius2 yielded more than 1400 different torsional conformers of butyronitrile. These were subsequently FF optimized to give two stable conformers of *gauche* and *anti* form of butyronitrile.
- [38] A.K. Rappe, C.J. Casewit, K.S. Colwell, W.A. Goddard-III and W.M. Skiff, J. Am. Chem. Soc. 114 (1992) 10024.
- [39] GRAMS/32 (r) Spectral Notebook v. 4.01A Galactic Industries Corporation Au: not cited. Please cite reference in text or delete from the list.